Fluxon dynamics in long Josephson junctions in the presence of a temperature gradient or spatial nonuniformity

Krasnov, V.M.; Oboznov, V.A.; Pedersen, Niels Falsig

Published in:
Physical Review B Condensed Matter

Link to article, DOI:
10.1103/PhysRevB.55.14486

Publication date:
1997

Document Version
Publisher's PDF, also known as Version of record

Fluxon dynamics in long Josephson junctions in the presence of a temperature gradient or spatial nonuniformity

V. M. Krasnov*
Department of Physics, Technical University of Denmark, DK-2800 Lyngby, Denmark
and Institute of Solid State Physics, Russian Academy of Sciences, 142432 Chernogolovka, Russia

V. A. Oboznov
Institute of Solid State Physics, Russian Academy of Sciences, 142432 Chernogolovka, Russia

N. F. Pedersen
Department of Physics, Technical University of Denmark, DK-2800 Lyngby, Denmark
(Received 15 July 1996; revised manuscript received 3 February 1997)

Fluxon dynamics in nonuniform Josephson junctions was studied both experimentally and theoretically. Two types of nonuniform junctions were considered: the first type had a nonuniform spatial distribution of critical and bias currents and the second had a temperature gradient applied along the junction. An analytical expression for the I-V curve in the presence of a temperature gradient or spatial nonuniformity was derived. It was shown that there is no static thermomagnetic Nernst effect due to Josephson fluxon motion despite the existence of a force pushing fluxons in the direction of smaller self-energy (from the cold to the hot end of the junction). A phenomenon, the ''zero crossing flux flow step'' (ZCFFS) with a nonzero voltage at a zero applied current, was observed in nonuniform long Josephson junctions. The phenomenon is due to the existence of a preferential direction for the Josephson vortex motion. ZCFFS's were observed at certain magnetic fields when the critical current in one direction but not the other becomes zero. Possible applications of nonuniform Josephson junctions in flux flow oscillators and as a superconducting diode are discussed.
[S0163-1829(97)06621-6]

I. INTRODUCTION

Properties of nonuniform Josephson junctions (JJ's) are of considerable interest both from the point of view of the various applications of such junctions in cryoelectronics and from the general scientific point of view. The nonuniformity in general means nonequal conditions for Josephson vortices in different parts of the junction and is typical for long JJ's even when it is not specially desired. It could be caused by the spatial variation of the critical current, the nonuniform current distribution, the nonrectangular shape of the junction, self-field effects, temperature gradients, trapped flux, and many other reasons.

However, the nonuniformity is sometimes introduced artificially in cryoelectronics, e.g., in the fabrication of the Josephson trigger with a special dependence of the critical current upon the magnetic field[1] and for suppression of Fiske resonances on I-V curves (IVC), which is important for the operation of various detectors (e.g., x-ray detectors[2,3] and flux-flow oscillators[4]). In flux-flow oscillators the nonuniformity is advantageously employed in order to reduce the self-field effect and to facilitate unidirectional fluxon motion.[4–6]

On the other hand, the problem of fluxon dynamics in nonuniform JJ's appears in the study of various fundamental physical phenomena. One of them is the problem of the transport entropy S_φ, and thermomagnetic effects observed not only for ordinary superconductors but also for highly anisotropic high-T_c superconductors (HTSC's);[7] these exhibit an intrinsic Josephson effect between individual superconducting layers[8] and thus are proven to have a quasi-two-dimensional (2D) layered structure with Josephson coupling between layers. Thermomagnetic effects were also observed for single superconductor–normal-metal–superconductor (SNS) JJ's (Ref. 9) and layered organic superconductors.[10] The thermomagnetic voltage is associated with the existence of a thermal force acting on the vortices. For example the Nernst voltage transversal to the temperature gradient is caused by the fluxon motion parallel to the temperature gradient under the thermal dragging force that could be expressed as $F_{\rm th}=-S_\varphi \nabla T$. The thermal force acting on Abrikosov vortices could be attributed to the scattering of quasiparticles on localized states in the vortex core[11,12] or the existence of a Lorentz force[13] and a Magnus force[10] caused by the counterflow mechanism.[14] However, for Josephson vortices in 2D layered superconductors and JJ's the situation is quite different. In superconductor-insulator-superconductor (SIS) structures, for example, the vortex does not have a normal core. The Magnus force approach also fails since Josephson vortices can not move across the junction. This is a reason for the absence of the Seebeck effect, i.e., the voltage along the temperature gradient in layered HTSC's, when the magnetic field is applied parallel to the layers.[15] Nevertheless some thermomagnetic effects might take place in SIS JJ's. The possibility of a Nernst effect due to the existence of the self-energy gradient of Josephson vortices in the presence of a temperature gradient was discussed in Refs. 16 and 17. However, some philosophical problems occur in this case, since Josephson vortices should move from the cold to the hot end of the junction, i.e., in the opposite direction compared to Abrikosov vortices, and the

energy will be transmitted from the cold to the hot end of the junction. This will violate the second law of thermodynamics unless an external energy source is involved. For SNS structures, on the other hand, the vortex has a normal core and a quasiparticle mechanism can cause a thermal force acting in the same direction as for Abrikosov vortices.

Thus by studying thermomagnetic effects in layered superconductors it might be possible to obtain important information about the structure of the vortex and the layered compound itself. There exist some evidence that several HTSC compounds may have SNS structure.[18–20] By studying thermomagnetic effects with a magnetic field applied parallel to the layers, it is possible, in principle, to decide whether the nature of intermediate layers in HTSC's are superconducting, normal, isolating, etc. Experiments with a temperature gradient applied to a single JJ are of great interest in understanding the thermomagnetic effects in layered superconductors, since they can provide the most explicit answer about the nature of the thermal force acting on Josephson vortices. In Ref. 21 the influence of the temperature gradient on a single SIS junction was studied. The Nernst effect was not observed in that case; however, the temperature gradient was shown to cause an asymmetry of I-V curves due to spatial variation of the viscosity. Yet the question whether the Nernst effect due to Josephson vortex motion could exist was not resolved.

In the present paper we have studied fluxon dynamics in nonuniform long JJ's, both theoretically and experimentally. Two types of nonuniform junctions were considered: the first type with an artificially made nonuniform spatial distribution of critical and bias currents (geometrical gradient) and the second type with a temperature gradient applied along the junction. It was shown that the force pushing fluxons towards the end with the smaller self-energy does not cause the fluxon motion from the cold to the hot end of the junction and thus there is no static Nernst effect in SIS JJ's. On the other hand, in the dynamic state this force can contribute to the asymmetry of IVC's. For both types of junctions unusual zero crossing flux flow steps (ZCFFS's) have been experimentally observed. Current-voltage characteristics of nonuniform junctions exhibit a nonzero voltage at a zero applied current. The phenomenon is due to the existence of a preferential direction for the Josephson vortex motion. ZCFFS's are observed at certain magnetic fields when the critical current in one direction but not the other becomes zero. An analytical expression for the I-V curve in the presence of a temperature gradient or spatial nonuniformity was derived. Possible applications of nonuniform Josephson junctions in flux flow oscillators and as a superconducting diode are discussed.

II. THEORY

Let us consider a one-dimensional nonuniform long JJ with a length L along the X axis. The magnetic field H is applied parallel to the JJ along the Y axis and the external bias current, with density J_e, is applied in the Z direction. A sketch of the JJ is shown in Fig. 1. When the magnetic field is applied, a screening current I_h is induced in the electrodes. Fluxon dynamics in a nonuniform junction can be described by the equation[1,22]

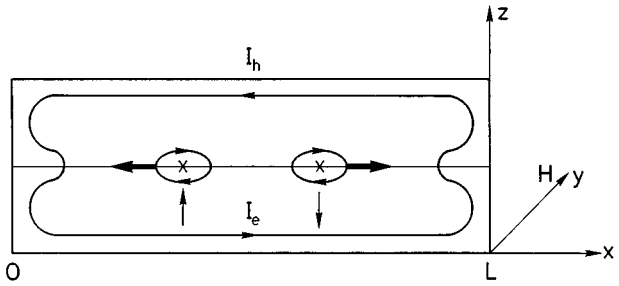

FIG. 1. A sketch of the Josephson junction. The direction of the Lorentz force acting on a positive fluxon for different directions of the bias current I_e is shown by thick arrows.

$$\left\{\frac{\partial}{\partial x}\left(J_c\lambda_J^2\frac{\partial}{\partial x}\right)-\frac{\Phi_0}{2\pi c}C\frac{\partial^2}{\partial t^2}-\frac{\Phi_0}{2\pi cR_N}\frac{\partial}{\partial t}\right\}\varphi(x,t)$$
$$=J_c\sin(\varphi)-J_e. \tag{1a}$$

In dimensionless units Eq. (1a) may be written as

$$\left\{\frac{\partial^2}{\partial\tilde{x}^2}-\frac{\partial^2}{\partial\tilde{t}^2}+\epsilon\frac{\partial}{\partial\tilde{x}}-\eta\frac{\partial}{\partial\tilde{t}}\right\}\varphi(\tilde{x},\tilde{t})=F[\sin(\varphi)-I_e]. \tag{1b}$$

Here $\varphi(x,t)$ is the phase difference, Φ_0 is a flux quantum, $\tilde{x}=x/\lambda_{J0}$, λ_{J0} is the normalization length equal to the Josephson penetration depth at some point of the junction, $\tilde{t}=(c_0/\lambda_{J0})t$, $c_0=(c/\sqrt{4\pi dC})=c\sqrt{(d_0/d\epsilon_r)}$ is the Swihart velocity, ϵ_r is the relative dielectric constant, $\eta=\lambda_{J0}/c_0CR_N$ is the viscosity coefficient, C is the junction capacitance per unit area, R_N is a quasiparticle resistance per unit area, $\epsilon=(\partial/\partial\tilde{x})(J_c\lambda_J^2)/J_c\lambda_J^2$, $F=\lambda_{J0}^2/\lambda_J^2$, $I_e=J_e/J_c$, $d=d_0+\lambda_1+\lambda_2$ is the magnetic thickness, $\lambda_{1,2}$ is the London penetration depth of electrodes, d_0 is the thickness of the tunnel barrier, and J_c, λ_J are spatially dependent values of the critical current density and the Josephson penetration depth, respectively, and $J_c=(c\Phi_0/8\pi^2d\lambda_J^2)$. Hereafter a ''tilde'' on a quantity implies that the quantity is measured in dimensionless units. The boundary conditions for Eq. (1) at $x=0$ and $x=L$ are

$$\frac{\partial\varphi}{\partial x}(0,t)=\frac{\partial\varphi}{\partial x}(L,t)=\frac{2\pi d}{\Phi_0}H. \tag{2}$$

The bias current acts on the fluxon with a Lorentz force

$$\mathbf{F}_L=(1/c)\mathbf{J}_e\times\mathbf{\Phi}_0, \tag{3}$$

as shown in Fig. 1. Below we will consider the different cases.

A. Steplike critical and bias current distribution (geometrical gradient)

First we will consider a long JJ with a steplike distribution of the critical current:

$$J_c(x)=\begin{cases}J_{c1}, & 0<x<x_1,\\ J_{c2}, & x_1<x<L;\end{cases}\quad \lambda_J(x)=\begin{cases}\lambda_{J1}, & 0<x<x_1,\\ \lambda_{J2}, & x_1<x<L;\end{cases}$$

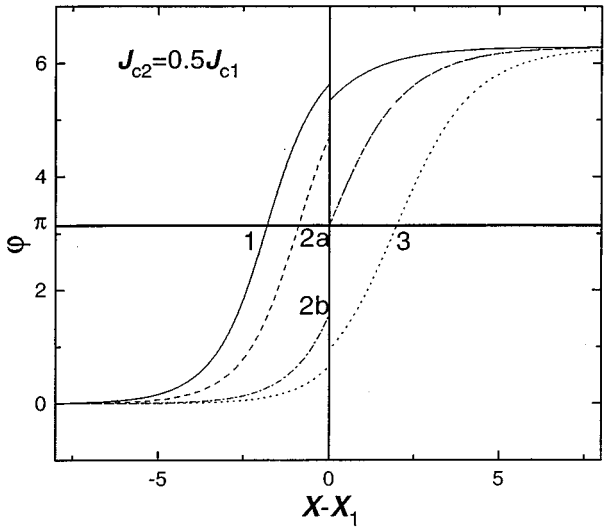

FIG. 2. Spatial dependence of the phase difference for a single fluxon in a junction with a steplike critical current distribution $J_{c2}=0.5J_{c1}$, for different positions of the fluxon center: (i) to the left of the boundary, curve 1, (ii) at the boundary, curves 2a and 2b, and (iii) to the right of the boundary, curve 3. It is seen that a switching from curve 2a to curve 2b occurs when the fluxon crosses the boundary $x=x_1$.

which is the simplest and the most illustrative type of nonuniformity.[22] In the static case the well-known single fluxon solution of Eq. (1) in both parts of the junction is

$$\varphi_0=4\arctan\left[\exp\left(\frac{x-a_i}{\lambda_{Ji}}\right)\right], \tag{4}$$

where the index $i=1,2$ corresponds to the different parts of the junction $0<x<x_1$ and $x_1<x<L$, respectively. Parameters a_i in Eq. (4) corresponding to the position of the fluxon center should be chosen from the condition of magnetic field continuity or the continuity of φ_x at $x=x_1$, Eq. (2). This gives

$$\lambda_{J1}\cosh[(x_1-a_1)/\lambda_{J1}]=\lambda_{J2}\cosh[(x_1-a_2)/\lambda_{J2}].$$

In Fig. 2 phase distributions for a junction with $J_{c2}=0.5J_{c1}$ are shown for different positions of the fluxon center: (i) to the left of the boundary $a_2<x_1$, curve 1, (ii) at the boundary $a_2=x_1$, curves 2a and 2b, and (iii) to the right of the boundary $a_2>x_1$,curve 3. It is seen that when the fluxon crosses the boundary a switching from $a_1<x_1$, curve 2a, to $a_1>x_1$, curve 2b, occurs in the left part of the junction.

The free energy of the junction is equal to

$$F=\int dx\,\frac{\varphi_0 J_c}{2\pi c}\left[\frac{(\varphi')^2\lambda_J^2}{2}+1-\cos\varphi\right]. \tag{5}$$

Thus when the fluxon crosses the boundary (curves 2a and 2b in Fig. 2) its self-energy is changed by the value

$$\Delta F=\frac{4\varphi_0 J_{c1}\lambda_{J1}}{\pi c}\sqrt{1-\frac{J_{c2}}{J_{c1}}}. \tag{6}$$

This energy drop means that there is an infinitely large force pushing the fluxon towards the region with the smaller critical current while infinitely large pinning prevents fluxon motion in the opposite direction.

The consideration above shows that the single fluxon state in the nonuniform junction with a steplike critical current distribution is not stable. Another possible way to satisfy the condition of the magnetic field continuity is to have several fluxons on the right side of the boundary. Then it is possible to avoid the free-energy discontinuity. Thus the stable static solution for a nonuniform junction corresponds to the case when the fluxon density is higher on the side with the smaller critical current. For example, the magnetic field penetrates into the junction in the form of a ''magnetic domain''[1] from that side of the junction.

The next consequence of a steplike critical current distribution is a complicated ''Fraunhofer pattern'' $I_c(H)$, see, e.g., Ref. 23. For example, if the ratio L/x_1 is an integer, there are two periods. The ordinary period $H_0=\Phi_0/dL$, corresponding to the entrance of an extra fluxon in the whole junction and the larger one H_1, corresponding to an integer number of fluxons in the smaller part of the junction, at which the critical current turns strictly to 0. Figure 3 shows the calculated $I_c(H)$ dependencies for a steplike critical current distribution with $J_{c2}=0.4J_{c1}$ and $x_1=0.1L$ and for different steplike bias current distributions $J_{e1}(x)=0\,\{0<x<x_2\}$, $J_{e2}\,\{x_2<x<L\}$ (see insets in Fig. 3), with $x_2=0$ (uniform bias) represented by open circles and $x_2=0.5L$ by solid triangles. The extra periodicity $H_1=10H_0$ is easily seen on the curves. The introduction of the bias current asymmetry results in an additional inclination of the $I_c(H)$ patterns. It is important that, due to the nonuniformity, minima of the critical current in positive and negative directions occur at different magnetic fields.

Another peculiar feature of the $I_c(H)$ pattern is the existence of a strong hysteresis due to the existence of extra pinning boundaries $x=x_1$, x_2 and the existence of multiple branches due to a possibility of several fluxon configurations matching the boundary condition. We have observed those features both in experiment and in numerical simulations—especially for rather long junctions.

B. Temperature gradient

We consider a long Josephson junction with a temperature gradient $\nabla T>0$ applied along the junction in the X-axis direction so that the left end of the junction ($x=0$) has a lower temperature T_1 than the right end ($x=L$), T_2, $T_1<T_2$. Local properties of the junction depend on temperature and thus on the coordinate. Let J_{c0}, λ_{J0} be the critical current and the Josephson penetration depth in the middle of the junction $x=L/2$ at the average temperature $T=T_0$.

The solution of Eq. (1b) can be found by perturbation theory.[24,17,22] We start from the frictionless motion of the Josephson vortex in a homogeneous junction ($\epsilon=\eta=f=0$). The single fluxon solution has a form of traveling wave (soliton):

$$\varphi_0=4\arctan(e^{\xi}), \tag{7}$$

where ξ,τ are the self-coordinates of the fluxon moving with the velocity v:

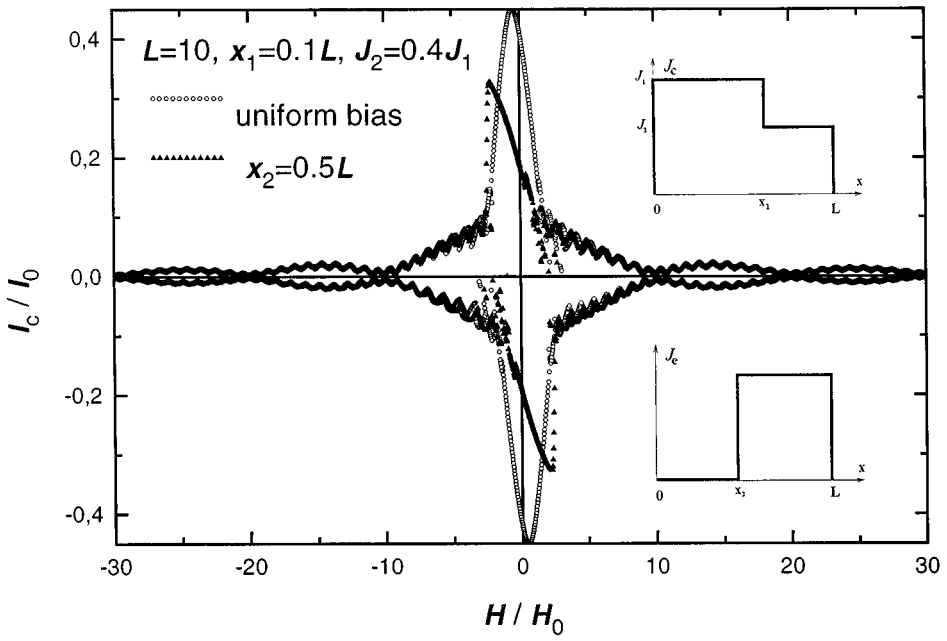

FIG. 3. Numerically calculated $I_c(H)$ dependencies for a steplike critical current distribution with $J_{c2}=0.4J_{c1}$ and $x_1=0.1L$ for uniform bias (open circles) and steplike bias current distribution (solid triangles) $J_{e1}(x)=0\,\{0<x<x_2\}$, $J_{e2}\{x_2<x<L\}$, $x_2=0.5$. Spatial distributions of the critical and bias currents are shown schematically in the insets.

$$\xi=\frac{\tilde{x}-\beta\tilde{t}}{\gamma},\quad \tau=\frac{\tilde{t}-\beta\tilde{x}}{\gamma},$$
$$\beta=\frac{v}{c_0},\quad \gamma=\sqrt{1-\beta^2}. \tag{8}$$

In the next approximation we consider the effect of finite viscosity, $\eta_0\neq 0$, $|\eta_0|\ll 1$, in a uniform junction ($\epsilon=f=0$). The solution of Eq. (2) is assumed to be of the form $\varphi_1=\varphi_0+\phi_1$, where $\phi_1\ll\varphi_0$. The well-known result for this case represents the appearance of a flux flow step (FFS) on the IVC:[25,26]

$$I_1=-\frac{4\beta\eta_0}{\pi\gamma}. \tag{9}$$

Finally we consider the effect of the temperature gradient. In the experimental situation the temperature difference on different sides of the junction is typically small, $T_2-T_1\ll T_0$, and spatially dependent parameters are defined as

$$\epsilon=\frac{\partial(J_c\lambda_J^2)}{J_c\lambda_J^2\partial\tilde{x}}=-\frac{\partial d}{d\,\partial\tilde{x}}\approx-\frac{\partial\lambda}{\lambda\,\partial T}\nabla T,$$
$$\frac{f}{\tilde{L}}=\frac{\partial(\lambda_{J0}^2/\lambda_J^2)}{\partial\tilde{x}}\approx-\frac{2\partial\lambda_J}{\lambda_J\partial T}\nabla T, \tag{10}$$
$$\eta_1=\tilde{L}\frac{\partial\eta}{\partial\tilde{x}}=\tilde{L}\frac{\partial\eta}{\partial T}\nabla T.$$

For a small temperature gradient we can use a linear approximation for the parameters in Eq. (10):

$$\epsilon\cong\text{const},\quad |\epsilon|\ll 1,$$
$$\eta\cong\eta_0+\eta_1\left(\frac{\tilde{x}}{\tilde{L}}-\frac{1}{2}\right),\quad |\eta_0|\ll 1,\quad |\eta_1|\ll|\eta_0|,$$
$$F\cong 1+f\left(\frac{\tilde{x}}{\tilde{L}}-\frac{1}{2}\right),\quad |f|\ll 1.$$

Coefficients ϵ, η_1, and f are constant and proportional to ∇T. We search for a solution in the form $\varphi_2=\varphi_1+\phi_2=\varphi_0+\phi_1+\phi_2$, $\phi_2\ll\varphi_0$. In coordinates (ξ,τ) Eq. (1b) may be rewritten as

$$\left\{\frac{\partial^2}{\partial\xi^2}-\frac{\partial^2}{\partial\tau^2}+\frac{\beta\eta+\epsilon}{\gamma}\frac{\partial}{\partial\xi}-\frac{\eta+\beta\epsilon}{\gamma}\frac{\partial}{\partial\tau}\right\}\varphi_2(\xi,\tau)$$
$$=(1+f)[\sin(\varphi_2)-I_e]. \tag{11}$$

Leaving only terms of the order of ϕ_2 in Eq. (11) we obtain

$$L_{\xi,\tau}\phi_2(\xi,\tau)=\left\{\frac{\partial^2}{\partial\xi^2}-\frac{\partial^2}{\partial\tau^2}+\frac{\beta\eta_0}{\gamma}\frac{\partial}{\partial\xi}-\frac{\eta_0}{\gamma}\frac{\partial}{\partial\tau}-\cos(\varphi_0)\right\}\times\phi_2(\xi,\tau)$$
$$=-\left\{\left[\frac{\epsilon}{\gamma}+\frac{\beta\eta_1}{\gamma}\left(\frac{\xi+\beta\tau}{\tilde{L}}-\frac{1}{2}\right)\right]\frac{\partial\varphi_0}{\partial\xi}-f\left(\frac{\xi+\beta\tau}{\tilde{L}}-\frac{1}{2}\right)\sin(\varphi_0)+I_2\right\}. \tag{12}$$

Performing the Fourier transformation of Eq. (12) and taking into account Eq. (7) we obtain

$$L_{\xi,\omega}\phi_2(\xi,\omega)=\left\{\frac{\partial^2}{\partial\xi^2}+2A\frac{\partial}{\partial\xi}+\omega^2-1+i\omega\frac{\eta_0}{\gamma}+\frac{2}{\cosh^2\xi}\right\}\times\phi_2(\xi,\omega).$$

Here $A=\beta\eta_0/2\gamma$. To transform the operator $L_{\xi,\omega}$ to the normal form we write the solution in the form $\phi_2=e^{-A\xi}\tilde{\phi}_2$. Then

$$L_{\xi,\omega}\phi_2(\xi,\omega)=\left\{\frac{\partial^2}{\partial\xi^2}+\Omega^2-1+\frac{2}{\cosh^2\xi}\right\}e^{-A\xi}\tilde{\phi}_2(\xi,\omega)$$
$$=\mathcal{F}_\omega(\mathrm{RHS}). \tag{13}$$
$$\Omega^2=\omega^2+i\omega\frac{\eta_0}{\gamma}-A^2.$$

Here $\mathcal{F}_\omega(\mathrm{RHS})$ is the short notation of the Fourier transform of the right-hand side of Eq. (12). The Green function of Eq. (13) is[26]

$$G_\Omega(\xi,\xi')=-\frac{\exp[-A(\xi-\xi')-Q|\xi-\xi'|]}{2Q(1-Q^2)}[\tanh(\xi)\pm Q]$$
$$\times[\tanh(\xi')\mp Q]. \tag{14}$$

Here the upper sign corresponds to the case $\xi>\xi'$, the lower sign to $\xi<\xi'$, and

$$Q=\begin{cases}\sqrt{1-\Omega^2}, & |\Omega|\leqslant 1,\\ -i\sqrt{\Omega^2-1}, & \Omega>1,\\ i\sqrt{\Omega^2-1}, & \Omega<-1.\end{cases}$$

Now to obtain ϕ_2 it is necessary to evaluate $\mathcal{F}_\omega(\mathrm{RHS})$. Here the problem is the appearance of the secular terms due to terms containing τ. To avoid this we take into account that when the stable flux flow state is achieved, the RHS of Eq. (12) is periodic in τ with the frequency $\omega_0=2\pi\tilde{v}/\tilde{L}$. Thus the τ containing terms have a saw-tooth-like form with the periodicity $\tau_0=\tilde{L}/\tilde{v}$. In other words, although the $\beta\tau$ terms in the RHS of Eq. (12) suggest linear growth of ϕ_2 with τ, this is not really the case since $\xi+\beta\tau=\gamma\tilde{x}$ [see the definition of Eq. (8)] which fixes the origin of spatial variations in Eq. (10). Thus the apparent secularity of $\beta\tau$ terms in Eq. (12) is merely a reflection of the $\tilde{x}$ dependence in Eq. (10).[27] The periodicity of the RHS of Eq. (12) means that if the fluxon enters the junction from one end at $\tau=\tau_1$ it will leave the junction from the other end and enter the junction from the initial point at $\tau=\tau_1+\tau_0$. Hence the right-hand side of Eq. (12) contains only a free term and harmonics of $n\omega_0$. Here we are interested in the dc characteristics of the Josephson junction so we will avoid oscillating harmonics.

Now it can be easily shown that the dc term of $\mathcal{F}_\omega(\mathrm{RHS})$ is

$$\mathcal{F}_\omega(\mathrm{RHS})=-2\pi\delta(\omega)\left[\frac{2\epsilon}{\gamma\cosh\xi}+2\left(\frac{\xi}{\tilde{L}}-\frac{1}{2}\right)\left(\frac{\beta\eta_1}{\gamma\cosh\xi}\right.\right.$$
$$\left.\left.+\frac{f\sinh\xi}{\cosh^2\xi}\right)+I_2\right]. \tag{15}$$

The solution of Eq. (12) is given by

$$\phi_2(\xi,\tau)=\frac{1}{2\pi}\int_{-\infty}^{+\infty}\int_{-\infty}^{+\infty}\mathcal{F}_\omega(\mathrm{RHS})(\xi',\omega)$$
$$\times G_\Omega(\xi,\xi')e^{i\omega\tau}d\omega d\xi'$$
$$\approx-\frac{e^{-A\xi}}{A^2\cosh\xi}\int_{-\infty}^{+\infty}\left[\frac{2\epsilon}{\gamma\cosh\xi'}+2\left(\frac{\xi'}{\tilde{L}}-\frac{1}{2}\right)\right.$$
$$\left.\times\left(\frac{\beta\eta_1}{\gamma\cosh\xi'}+\frac{f\sinh\xi'}{\cosh^2\xi'}\right)+I_2\right]\frac{e^{A\xi'}}{\cosh\xi'}d\xi'$$
$$\approx-\frac{e^{-A\xi}}{A^2\cosh\xi}\left[\frac{4\epsilon}{\gamma}-\frac{2\beta\eta_1}{\gamma}+\frac{f}{\tilde{L}}+\pi I_2\right].$$

In this equation we neglected terms of higher powers in A ($A\ll 1$). In order to have a finite value of $\phi_2(\xi,\tau)$ we require the value of the rectangular brackets to be equal to zero. Thus we obtain for the current I_2

$$I_2=-\frac{4\epsilon}{\pi\gamma}+\frac{2\beta\eta_1}{\pi\gamma}-\frac{f}{\pi\tilde{L}}. \tag{16}$$

The result of Eq. (16) can be also obtained by the method used in Ref. 24.[27] Assuming that the dc voltage is induced by the periodic change of the phase difference due to flux flow we may write

$$\beta=-\frac{V}{V_0},\quad V_0=\frac{\Phi_0 c_0}{Lc}. \tag{17}$$

We note that the limiting voltage V_0 in Eq. (17) is written for a single fluxon in the junction, Eq. (7). As a result, Eq. (16) is valid for low fluxon densities when interaction between fluxons can be neglected. In the case of arbitrary (but small) numbers of fluxons in the junction, V_0 should be replaced by $V_0'=hV_0$, where h is a real number representing the average number of fluxons in the junction. The total current is given by the sum of I_1 and I_2 and the I-V characteristic is

$$I=I_1+I_2=\frac{2(2\eta_0-\eta_1)V/V_0}{\pi\sqrt{1-(V/V_0)^2}}-\frac{4\epsilon}{\pi\sqrt{1-(V/V_0)^2}}-\frac{f}{\pi\tilde{L}}. \tag{18}$$

Finally we note that due to fluxon interaction with the edges of the JJ and with each other there is a certain lower threshold current for flux motion,[28] so that $V=0$ at $I=0$ in the IVC. Such effects were not taken into account in derivation of Eq. (18).

Let us consider the negative branch of the IVC, which corresponds to the motion of positive fluxons along the X axis. If the fluxon is moving from the cold to the hot end, we have $\eta_1>0,\epsilon<0$, $f<0$ and all the contributions to I_2 caused by the temperature gradient are positive, while $I_1<0$. In the opposite case when the fluxon is moving from the hot towards the cold end $\eta_1<0$, $\epsilon>0$, $f>0$, and both I_1 and I_2 are negative. The total IVC for both directions of the fluxon motion is shown in Fig. 4 for positive fluxons. The dotted curve in Fig. 4 represents a flux flow IVC in a uniform junction [Eq. (9)] $\eta_0=0.02$, $\epsilon=\eta_1=f=0$. The solid curve shows the IVC in the presence of a positive temperature

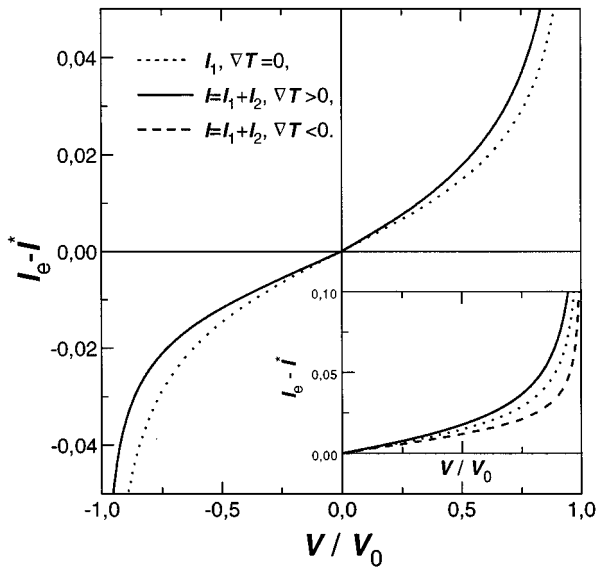

FIG. 4. The flux flow IVC of a long Josephson junction in a positive magnetic field without a temperature gradient (dotted curve), and with a positive temperature gradient along the junction (solid curve). The IVC's were shifted by $I^*=I(v=0)$, Eq. (18). In the inset flux flow IVC's are shown for a uniform junction $\nabla T=0$ (dotted curve) and for positive (solid curve) and negative (dashed curve) temperature gradients. Parameters were chosen for a typical experimental situation.

gradient $\nabla T=0.01$ [in dimensionless units $\nabla T=(\Delta T/T_c)/(L/\lambda_{J0})$]. Experimentally that corresponds to a gradient of approximately 2 K/cm in a Nb-based junction, $T_c\sim 9.2$ K with $L=10\lambda_J=500$ μm. In the inset of Fig. 4, flux flow steps are shown with $\nabla T=0$ (dotted curve) and with positive (solid curve) and negative (dashed curve) temperature gradients $|\nabla T|=0.01$. The dashed curve ($\nabla T=-0.01$) also represents the negative branch of the IVC with a positive temperature gradient ($\nabla T=0.01$, solid curve). Parameters $\epsilon=-0.0074$, $\eta_1=0.004$, and $f/\tilde{L}=-0.0083$ were chosen for $T_0/T_c=\frac{2}{3}$ ($\sim$6 K) and $\nabla T=0.01$($\sim$2 K/cm) using the definitions of Eq. (10). If the magnetic field changes sign and becomes negative, the asymmetry of flux flow steps also changes sign, since then the direction of fluxon motion is changed to the opposite, i.e., the positive current moves positive fluxons in the negative direction (against ∇T) while it moves negative fluxons in the positive direction (along ∇T), see Fig. 1 and Eq. (3).

From Fig. 4 it is seen that the temperature gradient influences the IVC of the junction in the following way. Flux flow steps on the IVC with $V<0$ and $V>0$ are asymmetric. The voltage at a certain current is higher when fluxons are moving from the cold to the hot end of the junction. The physical reason for the dependence of the IVC on the viscosity gradient term η_1 is the following. When the fluxon enters the junction from the cold end with the smaller viscosity it is accelerated faster than when it starts from the hot end.[21] The terms with ϵ and f are caused by a spatial variation of the critical current. This variation causes the appearance of a force associated with the gradient of the self-energy of the fluxon[16,17] pushing the Josephson vortex along the temperature gradient, i.e., from the cold to the hot end of the JJ and preventing motion in the opposite direction, as was discussed in Sec. II A with respect to the steplike critical current distribution. The self-energy force contributes to the anisotropy of the IVC by increasing the fluxon velocity when the fluxon is moving towards this force and by decreasing the velocity in the opposite case.

In Refs. 16 and 17 it was claimed that the self-energy force can cause the appearance of the thermomagnetic Nernst effect, i.e., generation of the voltage due to fluxon motion from the cold to the hot end of the junction in the opposite direction compared to the Abricosov vortex. Indeed, as soon as a single fluxon is placed in an infinitely long JJ so that there is no interaction with edges and other fluxons, then the self-energy force is the only force acting on the fluxon. Then the fluxon will move towards the region with smaller self-energy, i.e., from the cold to the hot end of the junction. A certain energy dissipation is associated with such motion. Moreover, the energy is transmitted by fluxons from the cold to the hot end of the junction. This is in clear contradiction with the second law of thermodynamics—claiming that such process can not take place without energy consumption. The clue to the paradox is in the fluxon interaction with the edges of the junctions. In order to organize the permanent flux flow we should introduce fluxons with some rate through the edges of the junction. As it was mentioned in the previous section in nonuniform junctions fluxons will penetrate into the junction from the side with the smaller critical current (hot side). To be able to move the fluxon from the cold to the hot side one should first spend the energy required for transportation of the fluxon towards the cold end with a larger fluxon self-energy. It is this energy that is released when the fluxon is moving towards the self-energy force. Thus without an energy supply $I=0$ such motion is impossible and there will be no Nernst voltage due to the Josephson vortex motion in the SIS junction.

Figure 5 illustrates the process of fluxon penetration into the nonuniform junction with increasing magnetic field at zero bias current. The data were obtained by numerical solution of Eq. (1), which automatically takes into account the fluxon interaction with the edges and with each other. The critical current distribution was taken to be linear and is shown in the top of the figure. The curves in the lower part of the figure represent the $\sin(\varphi)$ distribution inside the junction. The spatial coordinate is normalized to the Josephson penetration depth on the left side of the junction. The applied magnetic field is increasing from the top to the bottom curve. From Fig. 5 it is seen that fluxons penetrate the junction from the end with smaller critical current. The self-energy force directed from the left to the right prevents further penetration of fluxons inside the junction and causes a squeezing of the ''fluxon spring'' at larger magnetic fields. Thus in the conventional static experimental situation ($I=0$) when a uniform external magnetic field is applied to a nonuniform junction the magnetic field penetrates into the junction first from the side with a smaller critical current (hot side) in the form of a magnetic domain as was discussed in Sec. II A. The fluxon density in the domain changes in such a way that the Lorentz force $F_L=(1/4\pi)B(dH/dx)$ cancels the force F_{Jc}, associated with the variation of $J_c(x)$. Such behavior is well known with respect to the critical state in type-II superconductors.[18,29] A straightforward analogy is seen if

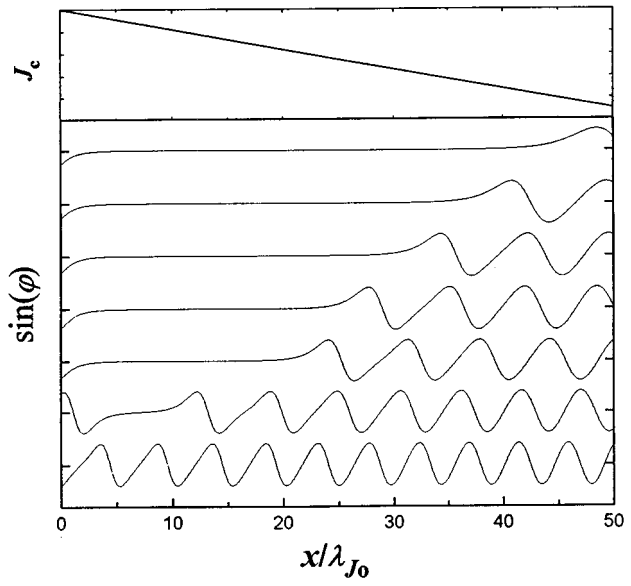

FIG. 5. Fluxon penetration into the nonuniform junction at zero bias current obtained by numerical solution of Eq. (1). The magnetic field is increasing from the top to the bottom curve. The critical current distribution is shown in the top of the figure. It is seen that fluxons penetrate the junction from the end with smaller critical current.

we consider F_{Jc} as a pinning force and the magnetic domain as the critical state of fluxons.

In Fig. 6 calculated dependencies $I_c(H)$ for a JJ with $\tilde{L}=10$ with and without a temperature gradient are shown. Figure 6 illustrates the existence of a static solution to Eq. (1) in the presence of a temperature gradient showing that the temperature gradient does not induce the flux motion itself and moreover that a certain critical current should be applied to start the flux motion. Thus in the conventional static case *there is no Nernst effect in the SIS JJ associated with a motion of Josephson vortices*. From Fig. 6 it is seen that with an applied temperature gradient the $I_c(H)$ dependencies for positive and negative current densities are shifted with respect to each other as was the case for a nonuniform critical current distribution (see Fig. 3). In general all the conclusions made in the previous section for a nonuniform critical current (penetration depth) distribution are valid qualitatively in the case with a temperature gradient. Besides, a spatial variation of the magnetic thickness d will cause additional nonuniform fluxon density distribution, so that the fluxon density will be larger at the hot end of the junction.

III. EXPERIMENT

I-V curves of long Josephson junctions were measured in a cryostat with a copper shield to screen electromagnetic waves, a double μ metal can for shielding the magnetic field, and a superconducting screen to avoid magnetic-field variation. The junction was placed in a He exchange gas so that the temperature could be changed in the range 4.2–20 K. Bias was provided by a low-noise analog dc current source and the voltage was either amplified by a low-noise amplifier or directly measured by an HP34420A nanovoltmeter. Experimental curves were plotted on an X-Y recorder.

A. Steplike critical and bias current distribution

In Fig. 7 the magnetic-field dependence of the critical current I_c for a Nb-AlO_x-Nb junction with $L=30\lambda_J$ is shown at $T=4.2$ K. The magnetic field is measured via the current through the magnet coil. Nb-AlO_x-Nb junctions were fabricated by sputter deposition and photolithography technology[30] at the Institute of Radio Engineering and Electronics, Moscow. The junctions were designed for measurements of the linewidth of a flux-flow oscillator and consist of two parts. The first part (''bias part,'' 90% of the junction) is connected to electrodes through which the external current is applied and the second part (''projection'' 10% of the junction) has no bias leads. The inset of Fig. 7 shows schematically the junction geometry. Two periods in the

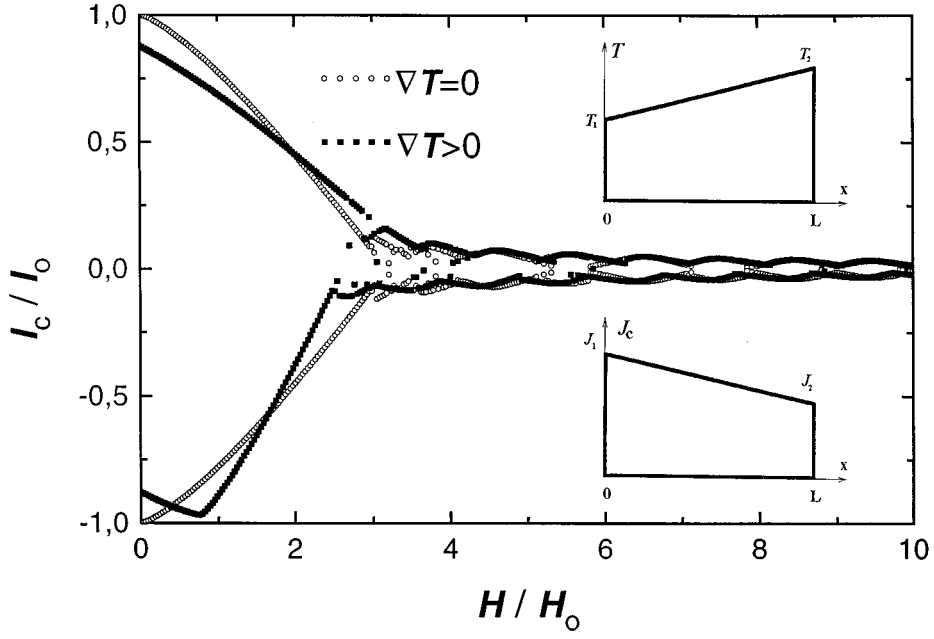

FIG. 6. Numerically calculated dependencies $I_c(H)$ for a long Josephson junction (i) without a temperature gradient (open circles) and (ii) with a temperature gradient ($\nabla T=0.02$) (solid squares). In the inset spatial distributions of the temperature and the critical current densities are shown schematically.

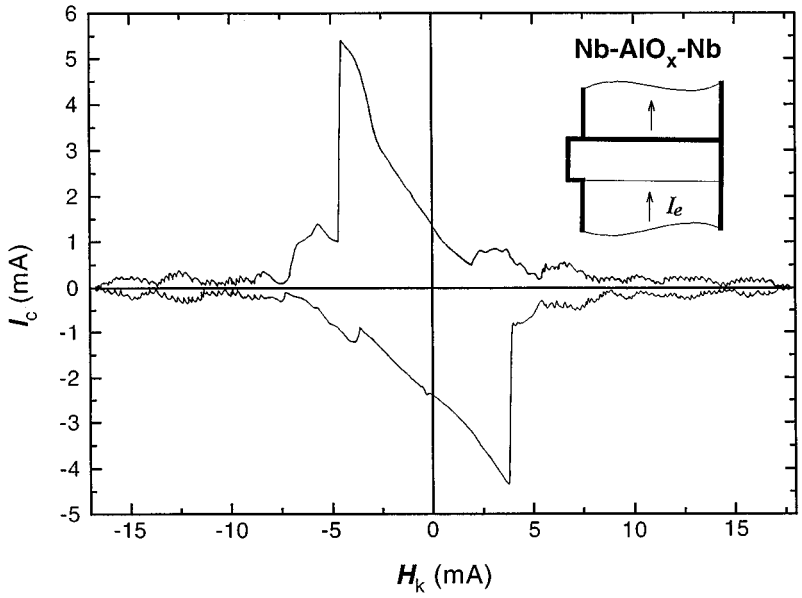

FIG. 7. Experimental dependence $I_c(H)$ for a Nb-AlO_x-Nb junction with $L=30\lambda_J$ at $T=4.2$ K. In the inset the junction geometry is shown schematically. Two periods in magnetic field are well defined, the larger period being about ten times the smaller one.

magnetic field are well defined in Fig. 7, the larger period being about 10 times the smaller one. It is also seen that minima of I_c for different current directions are shifted with respect to each other. The experimental $I_c(H)$ dependence is qualitatively the same as that in Fig. 3 and is thus well described by a steplike critical and bias current distribution. It is consistent with the second part of the JJ (10% of the length) having a larger critical current and the bias current mainly being injected through the first part. The sign of the magnetic field and distributions of critical and bias currents correspond to those in Sec. II A and Figs. 1 and 3.

1. Asymmetry of flux flow steps

Not only the critical current is asymmetric for this JJ. In Fig. 8, *I-V* curves for the same sample are shown at $H=3.0$ mA (solid curve) and $H=4.9$ mA (dotted curve). It is seen that FFS's clearly visible on the IVC's are highly asymmetric for positive and negative directions of the bias current. The positive bias FFS's are higher and more inclined than the negative bias FFS's. With a change of the direction of the magnetic field, the situation is reversed.

The nonuniformity of both the critical current and the bias current are responsible for this. The role of the nonuniform bias current was studied in detail in Ref. 5 and it was shown that nonuniform bias could cause FFS asymmetry of this type due to a self-field effect. We note, however, that the asymmetry of the IVC's observed in this sample is much larger than that for the junctions with the same geometry but with uniform critical current distribution.[30]

The asymmetry is most pronounced for the IVC at $H=3.0$ mA, for which there is no FFS for negative current and a quite large one for positive current. This curve most clearly illustrates the influence of the nonuniform critical current distribution which leads to nonuniform flux penetration into the JJ as discussed in Sec. II A. The magnetic field penetrates into the junction in the form of a magnetic domain through the end with the smaller critical current (the right end as shown in Fig. 3). The positive current pushes positive fluxons in the negative direction (to the left) and negative current to the right [see Fig. 1 and Eq. (3)]. At $H=3.0$ mA the domain did not reach the left end of the junction yet. Thus there are simply no fluxons in the left end that could be pushed by the negative current. On the other hand, there are fluxons on the right end of the junction that are driven to the left by the positive current, leading to the appearance of FFS's. This is also well seen from Fig. 7. At $H=3.0$ mA the junction is clearly in the Meisner state (without vortices) for the negative current and is in a mixed state (with vortices) for the positive current. In other words, the lower critical fields H_{c1} for the fluxon penetration are different for the left H_{c1L} and the right H_{c1R} sides of the junction due to nonuniform critical current distribution. The field $H=3.0$ mA is in between these two values, $H_{c1R}<H<H_{c1L}$. For larger magnetic fields the magnetic domain occupies the whole junc-

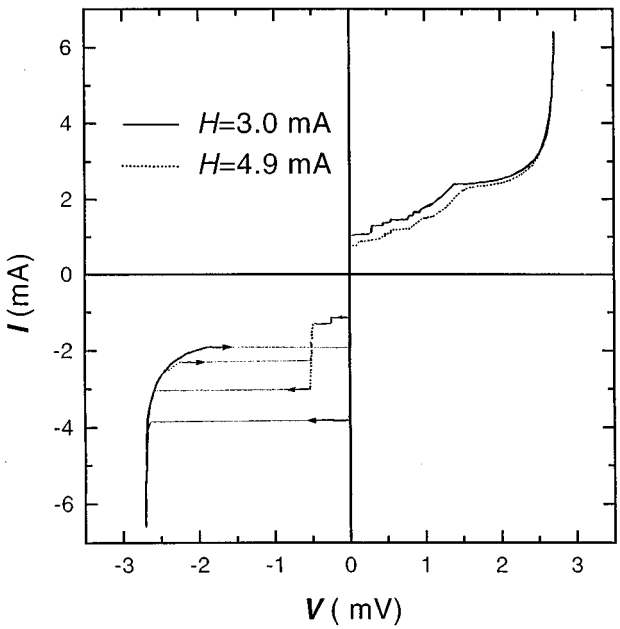

FIG. 8. Experimental *I-V* curves for the same Nb-AlO_x-Nb junction at two different magnetic fields and $T=4.2$ K. Asymmetry of FFS's for positive and negative directions of the bias current is clearly visible.

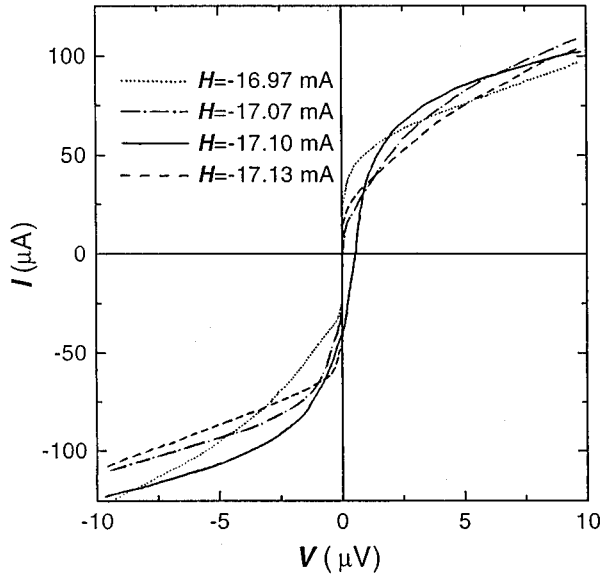

FIG. 9. Experimental I-V curves of the Nb-AlO_x-Nb junction in larger scale at $T=4.2$ K and for different magnetic fields near the field at which the critical current in one of the directions vanishes. A zero crossing flux flow step is observed at $H=-17.10$ mA (solid curve).

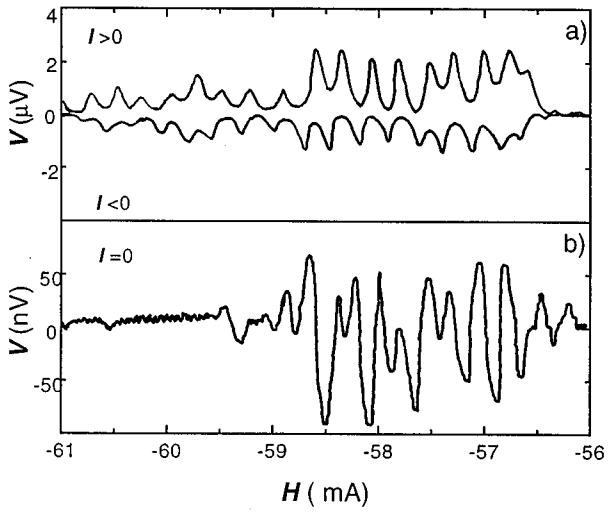

FIG. 10. Voltage across the Nb-AlO_x-Nb junction, biased with a constant current versus the applied magnetic field at $T=4.2$ K. (a) Two curves with a small positive (top) and small negative (bottom) bias current are shown. (b) The $V(H)$ dependence for zero applied current is shown providing a clear observation of the ZCFFS phenomenon. From (a) and (b) it can be seen that $I_c(H)$ patterns for positive and negative current are shifted with respect to each other and that ZCFFS's appear at the fields at which the critical current vanishes only in one direction.

tion; however, the additional asymmetry of FFS's due to different fluxon densities on different sides of the junction remains.

Nonuniform critical current distribution as well as nonuniform current bias can be responsible not only for the different heights of FFS's in different directions but also for the different inclination the steps. From Fig. 8 it is seen that the negative FFS's are much sharper than the positive FFS's. The reason is that for positive FFS's, when positive fluxons move to the left, they experience a strong pinning, while when they move in the opposite direction (negative FFS's) they are accelerated by the critical current decrease at the boundary $x=x_1$ [ϵ and f terms in Eqs. (1) and (18)].

2. Zero crossing flux flow steps

Under some conditions unusual zero crossing flux flow steps were observed in our nonuniform long JJ's. The phenomenon consists in the fact that the IVC of a nonuniform JJ can cross the $I=0$ axis at a nonzero voltage. In Fig. 9 I-V curves of the same Nb-AlO_x-Nb junction as in Figs. 7 and 8 are shown at a larger scale at $T=4.2$ K and for different magnetic fields near the field at which the critical current in one of the directions vanishes. The magnetic field is expressed via the current through the magnetic field coil. As we have already mentioned, the critical current of the junction is highly asymmetric. From Fig. 9 it is seen that for $H=-16.97$ mA critical currents in both directions are nearly equal. At $H=-17.07$ mA, I_c in the positive direction vanishes while in the negative direction it is not zero. ZCFFS is observed when the magnetic field is slightly increased. The solid curve in Fig. 9 shows IVC for $H=-17.10$ mA. It is seen that the IVC crosses the $I=0$ axis at a positive voltage of the order of half a microvolt. With a further increase of the magnetic field the ZCFFS disappears (see Fig. 9 for $H=-17.13$ mA). The IVC's shown in Fig. 9 are reproducible; however, a hysteresis with respect to the magnetic field reflects the hysteresis of $I_c(H)$ due to the existence of multiple branches as discussed above.

In general ZCFFS's were observed close to magnetic fields where I_c vanishes only in one direction. The sign of ZCFFS voltage corresponds to the sign of the critical current that vanished, e.g., in Fig. 9 the positive current turns to zero and a positive ZCFFS voltage is observed. This is illustrated in Fig. 10, where the voltage across the junction, biased with a constant current, is shown versus the applied magnetic field. The curves were plotted by sweeping the magnetic field. In Fig. 10(a) two curves with a small positive (top) and small negative (bottom) bias current are shown. Maximum/minimum of the voltage for positive/negative applied current are observed at fields at which the critical current $I_c(H)$ in the positive/negative direction reaches its minimum (zero) with a periodicity H_0. From Fig. 10(a) it is seen that minima of $I_c(H)$ for positive and negative current directions are shifted with respect to each other. An extra modulation of $V(H)$ is caused by the nonuniform critical current distribution and the existence of the larger period H_1(see Figs. 3 and 7). In Fig. 10(b) the $V(H)$ dependence for zero applied current is shown. In this case the junction was totally disconnected from a current source. Figure 10(b) yields a clear observation of the ZCFFS phenomenon. From Figs. 10(a) and 10(b) we observe that positive ZCFFS's appear in fields where the positive bias critical current vanishes [maximum of $V(H)(I>0)$, Fig. 10(a)] while the negative I_c does not. Similarly, negative ZCFFS's appear in fields where the negative bias critical current vanishes [minimum of $V(H)(I<0)$, Fig. 10(a)] and positive bias I_c does not. These conditions are fulfilled due to the shift of $I_c(H)$ dependencies for different bias directions, which in turn is caused by the non-

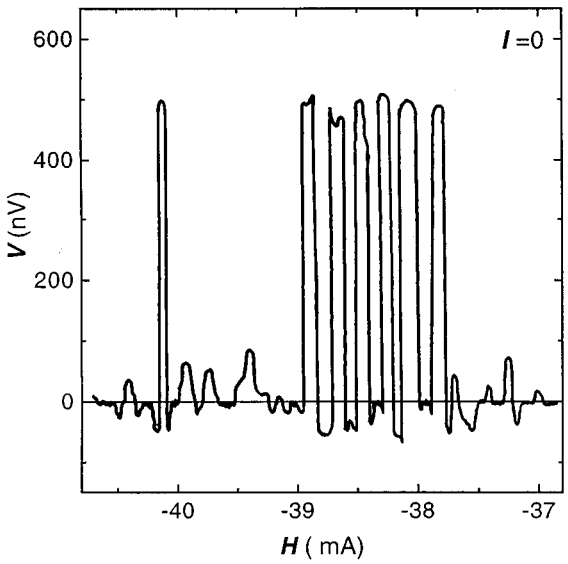

FIG. 11. The same as in Fig. 10(b) for different field range. It is seen that in addition to small oscillating ZCFFS's, large positive ZCFFS's with $V\sim 0.5$ μV are present corresponding to fluxon motion in the direction of smaller critical current.

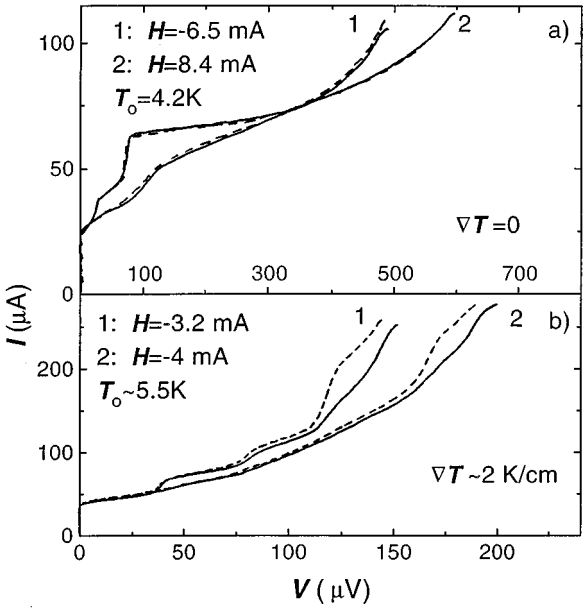

FIG. 12. Experimental flux flow IVC's for a Nb-NbO_x-Pb junction, $\tilde{L}\sim 8$, (a) without a temperature gradient at $T=4.2$ K, and (b) with $\nabla T\sim 2$ K/cm applied along the junction at the average temperature $T_0\sim 5.5$ K for different magnetic fields. Solid and dashed curves represent positive and negative branches of the IVC's, respectively. It is seen that the temperature gradient causes the asymmetry of IVC's so that the voltage is larger when fluxons move from the cold to the hot end of the junction.

uniformity of the junction. The shift of $I_c(H)$ naturally leads to an oscillatory behavior of the ZCFFS voltage as shown in Fig. 10(b). In the whole field range ZCFFS's reflect the modulation of $I_c(H)$. For example the absence of ZCFFS's for $-56<H<-53$ mA and $-62<H<-59$ mA is caused by the existence of the larger periodicity H_1, due to which $I_c(H)$ does not become zero at certain field intervals as shown in Figs. 3 and 7.

Another kind of ZCFFS is shown in Fig. 11. The curve was plotted in the same manner as that in Fig. 10(b). From Fig. 11 it is seen that in addition to small oscillating ZCFFS's, large positive ZCFFS's with $V\sim 0.5$ μV are present. Actually the solid curve in Fig. 9 corresponds to these large positive ZCFFS's. Comparison of the sign of the magnetic field and the generated ZCFFS voltage leads us to the conclusion that the positive ZCFFS's in Fig. 11 correspond to the motion of negative fluxons from the left to the right, i.e., in the direction of smaller critical current (see inset in Fig. 3).

B. Temperature gradient

Experiments with a temperature gradient applied along the junction were carried out on Nb-NbO_x-Pb junctions with overlap geometry. The junctions were fabricated on Si substrates 1.9×1.2 cm^2 by sputter deposition. One side of the substrate (1.2 cm) was attached to a massive copper block which was in good thermal contact with the He bath. The opposite side was attached to another copper block on which a heater was mounted. The copper blocks were thermally isolated from each other and placed in high vacuum to avoid parasitic external heat currents. When the heater was switched on the heat flows through the longer side of the substrate to the massive Cu block. Thus a temperature gradient was induced in the substrate and in the junction. The temperature was controlled by two thermometers placed on the Cu blocks and by a thermocouple directly on the substrate. A magnetic field parallel to the junction plane was created by a superconducting coil and measured via the current through the coil. The signs of the magnetic field and the temperature gradient correspond to that in Sec. II B and Figs. 1 and 6.

1. Asymmetry of flux flow steps

In Fig. 12 the IVC's for a Nb-NbO_x-Pb junction with a normalized length $\tilde{L}\sim 8$ are shown without a temperature gradient at $T=4.2$ K [Fig. 12(a)], and with $\nabla T\sim 2$ K/cm applied along the junction at the average temperature $T_0\sim 5.5$ K [Fig. 12(b)], for different magnetic fields. The solid and dashed curves represent positive and negative branches of the IVC's, respectively. From Fig. 12(a) it is seen that in the uniform case without a temperature gradient, flux flow steps on the IVC's are symmetrical for positive and negative current directions. On the other hand, when the temperature gradient is applied, an asymmetry of positive and negative branches of the IVC's appear. Positive IVC branches in Fig. 12(b) (solid curves) correspond to the motion of negative fluxons from the left to the right, i.e., along the temperature gradient from the cold to the hot end of the junction, see Figs. 1 and 6. Negative branches (dashed curves) correspond to fluxon motion in the opposite direction, i.e., from the hot to the cold end of the junction. The asymmetry changes sign when magnetic field changes sign as was discussed in Sec. II B. The experimental IVC's in Fig. 12(b) are in good qualitative agreement with the theoretical IVC's shown in the inset to Fig. 4 (solid and dashed curves) calculated approxi-

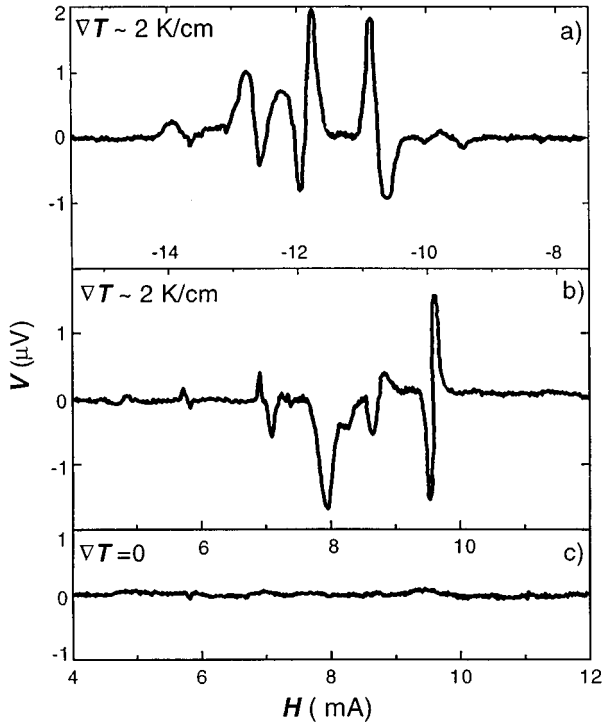

FIG. 13. Experimental dependencies $V(H)$ for the Nb-NbO_x-Pb junction for zero applied current and for different directions of the magnetic field. In (c) there is no temperature gradient and in (a) and (b) a temperature gradient of about 2 K/cm is applied while the mean temperature of the junction was about 5.5 K. It is seen that application of a temperature gradient causes generation of ZCFFS's.

mately for the experimental parameters of the junction and the temperature gradient. We note that the IVC's in Fig. 4 were calculated for the positive magnetic field while in Fig. 12(b) it is negative. Both experiment and theory show that the flux flow voltage is smaller when fluxons are moving from the hot to the cold end of the junction. We also note that both in the experiment (Fig. 12) and in theory (Fig. 4) FFS's for both bias current directions have the same limiting value V_0 [Eq. (17)] unlike that observed for the junction with nonuniform critical current distribution, Sec. III A 1, and in previous experiment.[21]

Another characteristic feature of Fig. 12(b) is that Fiske steps are more pronounced on the negative branches of the IVC (dashed curves) corresponding to the motion of negative fluxons from the hot to the cold end of the junction. A similar behavior was obtained in Ref. 21 from the computer simulation for the junction with spatial variation of the viscosity. The formation of Fiske steps (cavity resonances) is caused by the interference of moving fluxons with electromagnetic waves reflected from the boundary, where the fluxon leaves the junction. When fluxons leave the junction from the cold end with lower dissipation, the reflected waves have larger amplitude than when fluxons leave the junction from the end with larger dissipation (the hot end).[21] In addition the amplitude of reflected waves is larger when the fluxon leaves the junction from the end with larger critical current (the cold end) since the fluxon energy itself is larger on that end of the junction. Thus Fiske steps are more pronounced for fluxon motion from the hot to the cold end of the junction.

2. Zero crossing flux flow steps

In Fig. 13 experimental dependencies $V(H)$ for the same Nb-NbO_x-Pb junctions as in Fig. 12 are shown for zero applied current (the JJ is disconnected from the current source) and for different directions of the magnetic field. In Fig. 13(c) there is no temperature gradient and in Figs. 13(a) and 13(b) a temperature gradient of about 2 K/cm is applied while the mean temperature of the junction was about 5.5 K. From Fig. 13(c) it is seen that without a gradient ∇T, there is hardly any voltage generated at $I=0$, while from Figs. 13(a) and 13(b) it is seen that the application of a temperature gradient causes ZCFFS's. As in the case of Nb-AlO_x-Nb junctions with nonuniform $J_c(x)$ we can identify two features in ZCFFS's. (i) ZCFFS's are oscillating in sign with a periodicity of one flux quantum entering the junction and (ii) ZCFFS's are asymmetric, e.g., in Fig. 13(a) positive ZCFFS's have larger voltage while in Fig. 13(b) negative ZCFFS's have larger voltage, e.g., $H\sim 8$ mA there is a ZCFFS only of negative sign. Thus, as illustrated in Figs. 13(a) and 13(b), the asymmetry of ZCFFS's change sign with the magnetic field. For both directions of magnetic field, [Figs. 13(a) and 13(b)], the sign of ZCFFS's with larger voltage correspond to fluxon motion along the temperature gradient from the cold to the hot end of the junction.

IV. DISCUSSION

The necessary condition for observation of ZCFFS's is that the critical current vanishes in one direction and not in the other. Such a situation is possible in nonuniform JJ's due to a shift of Fraunhofer $I_c(H)$ patterns for different current directions as shown in Figs. 3 and 6. Taking into account that the Lorentz force [Eq. (3)], pushes fluxons in a particular direction (see Fig. 1) this means that the critical current for flux entry on one end of the junction is equal to zero and not on the other. This condition makes the direction from the end with $J_c(H)=0$ preferable for fluxon motion. Let us for definition suppose that the positive critical current is equal to 0 and the negative is not. This means that fluxons can freely enter the junction from the right side even when no external current is applied; on the other hand, there is a potential barrier for the fluxon entry from the left side. Thus preferential direction for fluxon motion is from right to left (negative X direction).

From Fig. 9 it is seen that the IVC's are rounded at magnetic fields close to that for which ZCFFS's are observed. Rounding of the IVC is a well-known consequence of fluctuations and noise in the JJ.[31] Taking into account that there is no barrier for fluxon entrance from the end of the junction with zero critical current density, even small fluctuations and noise will occasionally cause fluxon entrance from that end. On the average, fluxon motion from the end with $J_c(H)=0$ to the opposite end will occur, leading to formation of a ZCFFS. In other words we may say that nonuniform JJ behaves as a diode enabling unidirectional fluxon motion from the end with zero critical current and thus converting ac fluctuation and noise current to dc ZCFFS voltage. The second law of thermodynamics is not violated in this case, since the

energy is pumped out from fluctuations and noise. The mechanism of the formation of ZCFFS's is close to that for the formation of zero crossing Shapiro steps[32] although in the latter case the energy of external RF radiation is involved. There is, however, an important difference between these two phenomena, consisting in the fact that unlike zero crossing Shapiro steps ZCFFS's change sign with magnetic field. Namely the sign of the ZCFFS voltage is determined by the sign of vanishing critical current. This is well illustrated in Figs. 9 and 10. Since the formation of ZCFFS's depends on the $I_c(H)$ pattern, the dependence of the ZCFFS voltage on the magnetic field $V(H)$, should reflect the $I_c(H)$ dependence. In the case when $I_c(H)$ patterns for positive and negative current are shifted with respect to each other, which is the case for both types of nonuniformities considered here (see Figs. 3 and 6), oscillating $V(H)$ both of positive and negative sign should be observed. ZCFFS's of this type are seen in Fig. 10 as well as in Figs. 11 and 13.

Unlike zero crossing Shapiro steps ZCFFS's can be observed even without external electromagnetic power (noise). ZCFFS's could be caused by fluctuations or by other kinds of noise, e.g., by temperature or pressure variation. We note that special precautions were taken to reduce the noise in experimental setup. As can be seen from Figs. 10(b) and 13(c) the noise level is very low. For fluctuations-induced ZCFFS's the fluctuation energy should be compared with the Josephson coupling energy. When they are comparable fluctuations play a crucial role for the JJ. The Josephson coupling energy is proportional to the critical current. Thus when the critical current vanishes, the fluctuation energy exceeds the coupling energy and fluctuations cannot be neglected even though they were negligible for the maximum critical current at zero magnetic field. The importance of fluctuations at fields where $I_c(H)=0$ was discussed and studied previously; see, e.g., Ref. 31. Estimation of the temperature-induced fluctuation current amplitude gives about 1 μA. Although it is difficult to calculate the fluctuation-induced ZCFFS voltage in real experimental situation, we can evaluate its maximum value if we assume that the critical current is exactly 0 for one direction and nonzero for another. Then assuming that the IVC from the side with $J_c=0$ has the same shape as in Fig. 12(b) we can estimate the fluctuation-induced ZCFFS voltage to be of the order of 0.5 μV for our Nb-NbO_x-Pb junction. Taking into account that in Figs. 13(a) and 13(b) the magnetic field is about 3 times larger than in Fig. 12(b) we can also expect that maximum fluctuation-induced ZCFFS corresponding to Figs. 13(a) and 13(b) could be up to 1.5 μV which is in agreement with the observation in Fig. 13. This crude estimation shows that the fluctuation mechanism of the ZCFFS's formation could be important.

Another feature of ZCFFS's is the existing anisotropy for different signs of the voltage so that ZCFFS's of a definite voltage sign have a larger amplitude as seen in Figs. 11, 13(a), and 13(b). Such ZCFFS's correspond to fluxon motion towards the region with a smaller critical current, e.g., in the case of a temperature gradient, from the cold to the hot end of the junction. These ZCFFS's are presumably caused by the existence of an intrinsic force F_{Jc}, equal to a self-energy gradient of the fluxon. This force pushes the fluxon towards the region with a smaller critical current and prevents motion in the opposite direction. As it was shown above, this force strongly depends on the fluxon distribution and for a single fluxon in a junction with a steplike critical current the distribution could be infinitely large. For junctions with a smooth variation of the critical current the force is finite and is proportional to the derivative dJ_c/dx. As was discussed in Sec. II this force can contribute to the asymmetry of flux-flow voltage for different current directions. Indeed fluctuations/noise should spend more energy to move a fluxon to the end with higher critical current (cold end) than to the end with lower critical current (hot end). In other words, additional work against the self-energy force F_{Jc} should be done to move the fluxon from the hot to the cold end of the junction and motion in the opposite direction is preferential. Therefore ZCFFS's are asymmetric with ZCFFS's corresponding to fluxon motion towards the end with lower self-energy (from the cold to the hot end) having larger amplitude than ZCFFS's of the opposite sign. We note that the asymmetry of ZCFFS's are a reflection of the asymmetry of the IVC as shown in Figs. 4, 8, and 12. From Fig. 4 we can estimate this asymmetry to be about 20% which is in reasonable agreement with Figs. 13(a) and 13(b).

V. CONCLUSIONS

In conclusion, the fluxon dynamics in nonuniform Josephson junctions was studied both experimentally and theoretically. It was shown that nonuniformity causes asymmetry of IVC's and of $I_c(H)$ patterns so that positive and negative branches are shifted with respect to each other. Due to this, a phenomenon, ''zero crossing flux flow steps'' with a nonzero voltage at a zero applied current, can be observed in nonuniform long Josephson junctions. The phenomenon is due to the existence of a preferential direction for the Josephson vortex motion and the asymmetry of ZCFFS's can be due to the existence of a force pushing fluxons in the direction of smaller self-energy. ZCFFS's are observed at certain magnetic fields when the critical current in one of the directions becomes 0. The nonuniform long JJ in the ZCFFS state behaves as a diode enabling unidirectional fluctuation-driven fluxon motion in the direction from the end with zero critical current. Two types of nonuniform junctions were studied: the first type had a nonuniform spatial distribution of critical and bias currents and the second had a temperature gradient applied along the junction. Both types of junctions exhibit ZCFFS phenomena. By studying ZCFFS's caused by a temperature gradient we observed evidence for the existence of the thermal force pushing fluxons from the cold to the hot end of the junction. By direct numerical simulations it was shown, however, that this force itself does not cause flux motion since in conventional situations it is exactly balanced by the force caused by a nonuniform fluxon distribution. Thus there is no static Nernst effect associated with Josephson vortex motion in SIS JJ's. An analytical expression for the I-V curve in the presence of a temperature gradient or spatial variation of the junction parameters was derived; the theoretical IVC is in good qualitative agreement with the experiment.

Finally we discuss possible applications of nonuniform junctions in cryoelectronics. First, junctions with nonuniform $J_c(x)$ distribution might be promising objects for flux flow

oscillators. As it is seen from Fig. 8 introduction of nonuniform $J_c(x)$ makes flux flow steps corresponding to fluxon motion towards the end with lower critical current (negative branch in Fig. 8) sharper. This will make a flux flow oscillator more stable with respect to current fluctuation and could significantly reduce the linewidth of an oscillator. Another useful feature is a reduction of Fiske resonances on the same branch of the IVC corresponding to fluxon motion towards the end with larger dissipation and lower critical current (positive branch in Fig. 12). This could increase the tunability of the oscillator.

Another interesting application of such junctions is a superconducting diode. As it was shown, in nonuniform JJ's the ''Fraunhofer patterns'' $I_c(H)$ for positive and negative currents could be shifted with respect to each other. Thus, a situation when the critical current vanishes only on one end of the junction is possible. Under such conditions the nonuniform junction behaves as a fluxon diode enabling unidirectional fluxon motion from the end with zero $I_c(H)$. An important feature of such a diode is that it's direction can be controlled and could be changed to the opposite or modulated by a small magnetic field. Such a diode could be used in telecommunications, RSFQ logic, and other cryogenic applications.

ACKNOWLEDGMENTS

Stimulating discussions with G. Yu. Logvenov are gratefully acknowledged. The authors are grateful to V. P. Koshelets, L. V. Filippenko, and A. V. Shchukin for providing Nb-AlO_x-Nb junctions, to J. Mygind for his assistance in the experiment, to A. C. Scott and A. V. Ustinov for helpful discussions, and to I. Gabitov for valuable remarks. One of us (V.M.K.) is grateful to the Technical University of Denmark for hospitality. The work was supported in part by the Russian Foundation for Fundamental Research under Grant No. 96-02-19319.

*Present address: Department of Physics, Chalmers University of Technology, S-41296, Göteborg, Sweden. Electronic address: krasnov@fy.chalmers.se

[1] S. A. Vasenko, K. K. Likharev, and V. K. Semenov, Zh. Eksp. Teor. Phys. **4**, 1444 (1981).
[2] E. P. Houwman *et al.*, Physica C **183**, 339 (1991).
[3] S. Pagano *et al.*, in *Nonlinear Superconducting Devices and High- T_c Materials*, edited by R. D. Parmentier and N. F. Pedersen (World Scientific, Singapore, 1995), p. 437.
[4] J. H. Thompson, M. A. Ketkar, J. B. Beyer, and J. E. Nordman, IEEE Trans. Appl. Supercond. **3**, 2543 (1993).
[5] T. Nagatsuma, K. Enpuku, K. Sueoka, K. Yoshida, and F. Irie, J. Appl. Phys. **58**, 441 (1985).
[6] A. Benabdallah, J. G. Caputo, and A. C. Scott, Phys. Rev. B **54**, 16139 (1996).
[7] G. Yu. Logvenov, M. Hartman, and R. P. Huebener, Phys. Rev. B **46**, 11 102 (1992); H. C. Ri, R. Gross, F. Gollnik, A. Beck, R. P. Huebener, P. Wagner, and H. Adrian, *ibid.* **50**, 3312 (1994).
[8] R. Kleiner, F. Steinmeyer, G. Kunkel, and P. Mueller, Phys. Rev. Lett. **68**, 2394 (1992).
[9] G. Yu. Logvenov, V. A. Larkin, and V. V. Ryazanov, Phys. Rev. B **48**, 16 853 (1993).
[10] G. Yu. Logvenov, H. Ito, T. Ishiguro, G. Saito, S. Takasaki, J. Yamada, and H. Anzai, Physica C **264**, 261 (1996).
[11] J. Bardeen and M. J. Stephen, Phys. Rev. **140**, A1197 (1965); N. B. Kopnin and V. E. Kravtsov, Sov. Phys. JETP **44**, 861 (1976).
[12] E. Z. Meilikhov and R. M. Farzetdinova, Physica C **221**, 27 (1994).
[13] R. P. Huebener, A. V. Ustinov, and V. K. Kaplunenko, Phys. Rev. B **42**, 4831 (1990).
[14] V. L. Ginzburg, Sov. Phys. JETP **14**, 177 (1944).
[15] A. V. Samoilov, A. A. Yurgens, and N. V. Zavaritsky, Phys. Rev. B **46**, 6643 (1992).
[16] M. W. Coffey, Phys. Rev. B **48**, 9767 (1993).
[17] A. A. Golubov and G. Yu. Logvenov, Phys. Rev. B **51**, 3696 (1995).
[18] V. M. Krasnov, Physica C **190**, 357 (1992).
[19] A. A. Golubov and V. M. Krasnov, Physica C **196**, 177 (1992).
[20] A. Yurgens, D. Winkler, N. V. Zavaritsky, and T. Claeson, Phys. Rev. B **53**, R8887 (1996).
[21] G. Yu. Logvenov, I. V. Vernik, M. T. Goncharov, H. Kohlstedt, and A. V. Ustinov, Phys. Lett. A **196**, 76 (1994).
[22] S. Sakai, M. R. Samuelsen, and O. H. Olsen, Phys. Rev. B **36**, 217 (1987); Y. S. Kivshar and B. A. Malomed, J. Appl. Phys. **65**, 879 (1989); M. F. Petras and J. E. Nordman, Phys. Rev. B **39**, 6492 (1989).
[23] A. Barone and G. Paterno, *Physics and Applications of the Josephson Effect* (Wiley, New York, 1982).
[24] D. W. McLaughlin and A. C. Scott, Phys. Rev. A **18**, 1652 (1978).
[25] P. M. Marcus and Y. Imry, Solid State Commun. **33**, 345 (1980).
[26] M. B. Mineev, G. S. Mkrtchyan, and V. V. Shmidt, J. Low Temp. Phys. **45**, 497 (1981).
[27] A. C. Scott (private communication).
[28] N. F. Pedersen, M. R. Samuelsen, and D. Welner, Phys. Rev. B **30**, 4057 (1984).
[29] A. Campbell and J. Evetts, Adv. Phys. **21**, 199 (1972).
[30] V. P. Koshelets, S. A. Kovtonyuk, I. L. Serpuchenko, L. V. Filippenko, and A. V. Shchukin, IEEE Trans. Magn. **MAG-27**, 3141 (1991).
[31] J. T. Anderson and A. M. Goldman, Physica **55**, 256 (1971).
[32] M. T. Levinsen, R. Y. Chiao, M. J. Feldman, and B. A. Tucker, Appl. Phys. Lett. **31**, 776 (1977).